Available online at www.sciencedirect.com
SCIENCE DIRECT®
PERGAMON
Polyhedron 22 (2003) 2091–2098
POLYHEDRON
www.elsevier.com/locate/poly

Heat capacity study of the doping effect of paramagnetic impurity in organic spin-Peierls system: *p*-CyDOV radical crystal

K. Mukai [a,*], M. Yanagimoto [a], S. Tanaka [b], M. Mito [b], T. Kawae [b], K. Takeda [b]

[a] *Faculty of Science, Department of Chemistry, Ehime University, Bunkyo-cho, Matsuyama 790-8577, Japan*
[b] *Institute of Environmental Systems, Graduate School of Engineering, Kyushu University, Fukuoka 812-8581, Japan*

Received 6 October 2002; accepted 30 January 2003

Abstract

Heat capacity studies were performed for the doped verdazyl radical crystals, $(p\text{-CyDOV})_{1-x}(p\text{-CyDTV})_x$ ($x = 0$, 0.01, and 0.07), to clarify the effect of magnetic impurity (*p*-CyDTV) on the spin-Peierls (SP) transition ($T_{SP} = 15.0$ K) of 3-(4-cyanophenyl)-1,5-dimethyl-6-oxoverdazyl (*p*-CyDOV) radical crystal, where the >C=O group in *p*-CyDOV is replaced by the >C=S group in *p*-CyDTV. The antiferromagnetic (AFM) transitions were observed at $T_N = 0.135$, 0.290, and 0.164 K for the crystals with $x = 0$, 0.01, and 0.07, respectively, indicating the coexistence of AFM order and SP state in the systems with $x = 0$ and 0.01, and the appearance of the single phase of AFM order in the system with $x = 0.07$ below $T_N = 0.164$ K. However, the heat capacity anomaly associated with the SP transition was not found at $T_{SP} = 15.0$ K for the pure *p*-CyDOV crystal ($x = 0$), whereas the anomalous broad peak in the heat capacity was observed at $T'_{SP} = 5.6$ K. The entropy consumption in the above broad peak was about 3% of the total spin entropy R ln 2, suggesting that this transition may relate to SP transition. The pressure induced by the solidification of the Apiezon-N grease, which was used as the thermal binder for the heat capacity measurement, at low temperature may affect the shift of the SP transition temperature. The doping effects for the organic SP system (*p*-CyDOV), which include the temperature (T: T_{SP} and T_N)—impurity (x) phase diagram, are similar to those for the inorganic SP system ($CuGeO_3$), although the one-dimensionality, i.e., $|zJ'/J| \cong 6 \times 10^{-4}$, in the organic *p*-CyDOV system is much higher than that ($\sim 10^{-1}$) in the inorganic $CuGeO_3$ system, where zJ' and J are inter- and intra-chain exchange interactions. This work is the first report of the heat capacity study of the doping effect on the organic SP transition system.

Keywords: Verdazyl radical; Spin-Peierls transition; Heat capacity; Magnetism; Doping effect; Antiferromagnetic order; High-field magnetization

1. Introduction

The spin-Peierls (SP) transition is well known as one of the most interesting magnetic behaviors observed for organic radical salts, such as TTF-CuBDT and MEM-$(TCNQ)_2$ [1–3]. The SP transition occurs when a system of uniform antiferromagnetic (AFM) Heisenberg linear chains undergoes a transformation to a system of dimerized or alternating AFM linear chains, due to spin-phonon coupling between the one-dimensional (1D) spin and the 3D phonon systems. Below the transition temperature (T_{SP}), the ground state is spin singlet (nonmagnetic), and a finite energy gap opens in the excitation spectrum. The most striking feature in SP transition is that the magnetic susceptibilities exponentially drop to zero below T_{SP}. The SP transition was also observed for the inorganic compound $CuGeO_3$ ($T_{SP} =$ 14.2 K) [4,5].

The doping effects of magnetic (Mn^{2+} ($S = 5/2$) [6], Ni^{2+} ($S = 1$) [6,7] and Co^{2+} ($S = 3/2$) [8]), and nonmagnetic (Zn^{2+} ($S = 0$) [5,7,9,10] and Mg^{2+} ($S = 0$) [7,11,12]) impurities have been studied for the SP transition of $CuGeO_3$ (Cu^{2+} ($S = 1/2$)). Similar studies have been performed for the Si-doped $CuGeO_3$ ($CuGe_{1-x}Si_xO_3$) [6,10,13–15]. The SP transition temperature ($T_{SP} = 14.2$ K) decreased rapidly by increasing the concentration (x) of impurities and disappeared at around $x = 0.01$–0.04 depending on the kinds of impurities. Further, it has been found that the AFM phase

* Corresponding author. Tel.: +81-89-927-9588; fax: +81-89-927-9590.
E-mail address: mukai@chem.sci.ehime-u.ac.jp (K. Mukai).

0277-5387/03/$ - see front matter © 2003 Elsevier Science Ltd. All rights reserved.
doi:10.1016/S0277-5387(03)00244-4

transition appears in the doped SP systems below 5 K, and the AFM long-range order and SP state coexist in the doped SP systems below the critical concentration (x_C).

As reported in a previous work, the magnetic susceptibility (χ_M) of organic neutral verdazyl radical crystal, 3-(4-cyanophenyl)-1,5-dimethyl-6-oxoverdazyl (p-CyDOV) (Fig. 1), with $S = 1/2$ exhibits the characteristic properties of the SP transition [16,17]. The χ_M of p-CyDOV shows a broad maximum at 54 K, and decreases abruptly at SP transition temperature $T_{SP} = 15.0$ K. The susceptibility above 15.0 K can be well explained by the 1D Heisenberg linear-chain model [18] with AFM exchange interaction of $2J/k_B = -84$ K between neighboring spins. The magnetic energy gap $\Delta(0)$ at $T = 0$ K and the spin–lattice coupling constant λ calculated from T_{SP} and $2J/k_B$ are 26 K and 0.33, respectively [16]. High-field magnetization data ($H = 0$–35 T) that provide clear evidence for a SP transition were reported, and the magnetic phase diagram was determined for the p-CyDOV crystal [17].

The doping effects of magnetic (p-CyDTV and p-BrDOV) and nonmagnetic (p-CyDOV-H) impurities have been studied for the SP transition of p-CyDOV, where the $>$C=O group in p-CyDOV is replaced by the $>$C=S group in p-CyDTV, the CN group in p-CyDOV is replaced by the Br group in p-BrDOV, and the p-CyDOV-H is a reduced form of p-CyDOV [19–22]. The T_{SP} of the doped crystals, $(p\text{-CyDOV})_{1-x}(p\text{-CyDTV})_x$, $(p\text{-CyDOV})_{1-x}(p\text{-BrDOV})_x$, and $(p\text{-CyDOV})_{1-x}(p\text{-CyDOV-H})_x$ ($x = 0$–0.10), decreased rapidly by increasing the concentration (x) of impurities and the SP state disappeared at around $x = 0.03$–0.07 depending on the kinds of impurities [19–21]. However, the clear detection of the AFM transition in the SP phase has not been reported for the present systems at low temperatures.

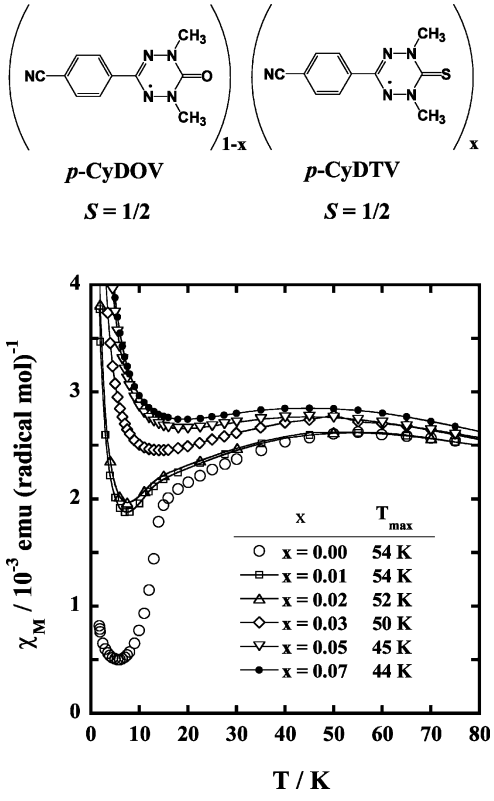

Fig. 1. Magnetic susceptibility ($\chi_M(x, T)$) of the doped p-CyDOV radical system, $(p\text{-CyDOV})_{1-x}(p\text{-CyDTV})_x$ ($x = 0$–0.07), in the temperature range of 1.8–80 K.

In the present work, the measurements of the temperature dependence of the heat capacity (0.10–32 K) of the doped crystals, $(p\text{-CyDOV})_{1-x}(p\text{-CyDTV})_x$ ($x = 0$, 0.01, and 0.07), were performed to study the effects of p-CyDTV on the SP system: p-CyDOV. The present work provides the first example of the heat capacity study of the doping effect of magnetic impurity on the organic SP system.

2. Experimental

p-CyDOV and p-CyDTV were prepared according to the method of Neugebauer et al. [23]. Preparation of the powder samples of doped p-CyDOV crystals, $(p\text{-CyDOV})_{1-x}(p\text{-CyDTV})_x$ ($x = 0$, 0.01, and 0.07), were reported in a previous work [19].

Measurements of the heat capacity, C_P, were performed for the doped radical crystals in the temperature range of 0.1–32 K, using the usual type of adiabatic calorimeter described previously in detail [24]. The measurements were performed on 0.497 g ($x = 0$), 0.540 g ($x = 0.01$), and 0.495 g ($x = 0.07$) powder samples mixed with the thermal binder Apiezon-N grease (0.467, 0.418, and 0.976 g), respectively. The data were corrected for the heat capacity of the addenda: in the case of $x = 0$, the heat capacity of the addenda (Cu platform, Apiezon-N grease etc.) was about 5% at 5 K and 76% at 15 K for the total heat capacity, for instance.

3. Results

3.1. Previous study of the crystal structure and magnetic property of the doped-radical crystals, $(p\text{-CyDOV})_{1-x}(p\text{-CyDTV})_x$

The Debye–Scherrer X-ray diffraction pattern of the p-CyDOV radical crystal ($x = 0$) is quite different from that of the p-CyDTV crystal ($x = 1$), as reported in a previous work (see Fig. 3 in Ref. [19]). However, the X-ray diffraction patterns of doped-radical crystals with $x = 0.01$, 0.02, 0.03, 0.05, and 0.07 are quite similar to that of the pure p-CyDOV crystal ($x = 0$). The diffraction pattern due to p-CyDTV crystal was not observed for the doped-radical crystals ($x = 0.01$–0.07). The

result indicates that the dopant molecules homogeneously distribute in the AFM chains of the *p*-CyDOV in each sample, and the crystal structure of doped-radical crystals ($x = 0.01$–0.07) is almost the same as that of the pure *p*-CyDOV ($x = 0$) at room temperature [19].

The susceptibility of the dopant *p*-CyDTV radical crystal follows a Curie–Weiss law with a Weiss constant of $\theta = -3.8$ K [19]. The susceptibilities of the doped radical crystals ($x = 0$–0.07) have also been studied in a previous work (see Fig. 2 in Ref. [19]), and the same figure is shown in Fig. 1. The susceptibility of each doped crystal shows a broad maximum at the temperature of T_{max}. The value of T_{max} decreases as the concentration (x) of *p*-CyDTV increases. The SP transition indicated by a drop of χ_M near 13–15 K was observed in the samples with $x \leqq 0.02$. The values of T_{max} and T_{SP} are listed in Table 1.

The temperature dependence of $\chi_M(x, T)$'s above T_{SP} can be simply described by the sum of the two contributions; one is from the 1D-Heisenberg AFM linear-chain system ($\chi_{1D\text{-}HAF}(T)$) with corrected T_{max}^{Corr} values and the other is a paramagnetic contribution ($\chi_{Curie}(T)$).

$$\chi_M(x, T) = C_{1D\text{-}HAF}(x)\chi_{1D\text{-}HAF}(T) + C_{Curie}(x)\chi_{Curie}(T) \quad (T > T_{SP}) \tag{1}$$

where $C_{1D\text{-}HAF}(x) + C_{Curie}(x) = 1$, and $\chi_{Curie}(T)$ is given by $\chi_{Curie}(T) = N_O g^2 \mu_B^2 S(S+1)/3k_B T$ with $S = 1/2$. The T_{max}^{Corr}, $2J/k_B$, $C_{1D\text{-}HAF}(x)$, and $C_{Curie}(x)$ values obtained are listed in Table 1.

On the other hand, the $\chi_M(x, T)$'s of the doped radical crystals with $x = 0.01$–0.07 below T_{SP} were described by three terms [11,19]:

$$\chi_M(x, T) = C_{SP}(x)\chi_{SP}(T) + C_{1D\text{-}HAF}(x)\chi_{1D\text{-}HAF}(T) + C_{Curie}(x)\chi_{Curie}(T) \quad (T < T_{SP}) \tag{2}$$

where $C_{SP}(x) + C_{1D\text{-}HAF}(x) + C_{Curie}(x) = 1$, and $\chi_{Curie}(T)$ in Eq. (2) is the same as that in Eq. (1). The second term represents the contribution from 1D-Heisenberg AFM linear-chain (1D-HAF) subsystem. The susceptibility for the SP state ($\chi_{SP}(T)$) was calculated from the $\chi_M(x, T)$ for the pure *p*-CyDOV ($x = 0$) below T_{SP} by using Eq. (2), by assuming that the fraction $C_{1D\text{-}HAF}(0) = 0$ for $x = 0$. The $C_{SP}(x)$, $C_{1D\text{-}HAF}(x)$, and C_{Curie} values obtained are listed in Table 1.

Recently, the measurements of the field dependence of magnetization ($H = 0$–55 T) were performed for the doped verdazyl radical crystals, $(p\text{-CyDOV})_{1-x}(p\text{-CyDTV})_x$ ($x = 0$, 0.01, 0.02, 0.03, 0.05, and 0.07) [25]. We have found that the high-field magnetization $M(x, H)$ curves of the doped organic SP system below $T_{SP} = 15.0$ K can be well explained by the sum of the magnetization (M) of the SP state ($C_{SP}(x)M_{SP}(H)$),

Table 1
Magnetic properties of the doped-radical crystals, $(p\text{-CyDOV})_{1-x}(p\text{-CyDTV})_x$ ($x = 0$–0.07)

x	T_{max} (K)	T_{max}^{Corr} (K)	$2J/k_B$ (K)	zJ'/k_B (K)	T_{SP} (K)	T_{SP}' (K)	T_N (K)	C_{Curie}	C_{SP} ($T < T_{SP}$)	$C_{1D\text{-}HAF}$ ($T < T_{SP}$)	$C_{1D\text{-}HAF}$ ($T > T_{SP}$)
0	54	54	−84.2		15.0	5.6	0.135	0.004	0.996	0	0.996
0.01	54	55	−85.8		13.5	5.3	0.290	0.011	0.448	0.541	0.989
0.02	52	55	−85.8		13.0			0.012	0.406	0.582	0.988
0.03	50	53	−82.7					0.019		0.981	0.981
0.05	45	52	−81.1					0.024		0.976	0.976
0.07	44	52	−81.1 (−72.0) [a]	−0.025			0.164	0.025		0.975	0.975

[a] The value determined by the heat capacity measurement.

1D Heisenberg antiferromagnet ($C_{1D\text{-}HAF}(x)M_{1D\text{-}HAF}(H)$), and Curie impurity ($C_{Curie}(x)M_{Curie}(H)$),

$$M(x,\ H) = C_{SP}(x)M_{SP}(H) + C_{1D\text{-}HAF}(x)M_{1D\text{-}HAF}(H) + C_{Curie}(x)M_{Curie}(H) \quad (3)$$

where $C_i(x)$ is the fraction of the ith contribution. The result suggests the coexistence of SP state and AFM long-range order in the doped p-CyDOV radical system at low temperature.

3.2. Measurement of the heat capacity

The temperature dependence of the heat capacity, C_P, of the doped p-CyDOV radical crystals ($x = 0$, 0.01, and 0.07) is shown in Fig. 2 (0.10–32 K) and Fig. 3 (0.10–2.0 K). The pure p-CyDOV crystal with $x = 0$ and the doped crystal with $x = 0.01$ show SP transition at $T_{SP} =$ 15.0 and 13.5 K, respectively, as shown in Fig. 1 [19]. Consequently, we may expect heat capacity anomalies at the T_{SP} for these crystals [3,26]. However, such anomalies were not observed for the crystals ($x = 0$ and 0.01) around T_{SP}, as we can see from the results shown in Fig. 2. Instead of the above expectation, we found heat capacity hump at $T'_{SP}(0) = 5.6$ K and $T'_{SP}(0.01) = 5.3$ K with the magnetic entropy consumption up to 3 and 1%, respectively, as shown in Figs. 4 and 5. While any hump was not seen for the $x = 0.07$ system in this temperature region. On the other hand, as shown in Fig. 3, the heat capacities of the pure p-CyDOV ($x = 0$) and the doped radical crystals ($x = 0.01$ and 0.07) exhibit a sharp λ-like peak at $T_N = 0.135 \pm 0.002$, 0.290 ± 0.002, and 0.164 ± 0.002 K, respectively, indicating a 3D magnetic phase transition. The values of T_N and C_P do not give a systematic change against the dopant concentration (x); we will discuss this point later.

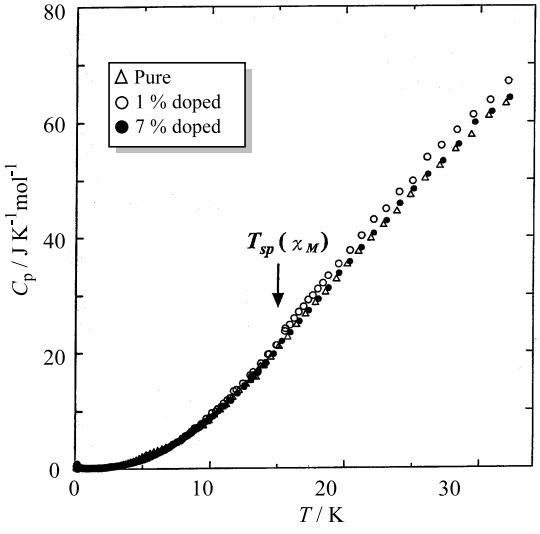

Fig. 2. Heat capacity (C_P) of the doped p-CyDOV radical system, $(p\text{-CyDOV})_{1-x}(p\text{-CyDTV})_x$ ($x = 0$, 0.01 and 0.07), in the temperature range of 0.10–32 K.

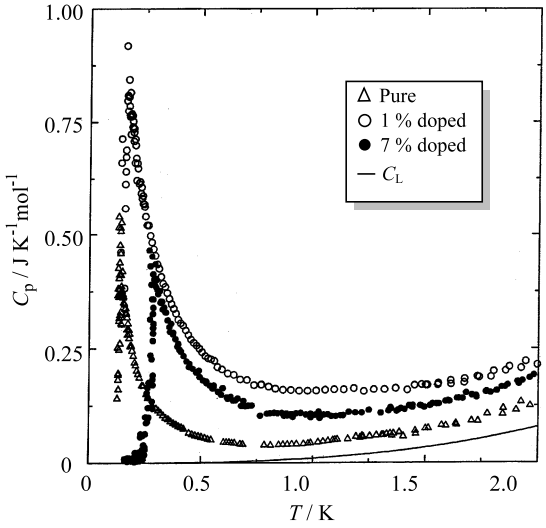

Fig. 3. Heat capacity (C_P) of the doped p-CyDOV radical system, $(p\text{-CyDOV})_{1-x}(p\text{-CyDTV})_x$ ($x = 0$, 0.01 and 0.07), in the temperature range of 0.10–2.0 K. The solid line is the estimated lattice contribution C_L.

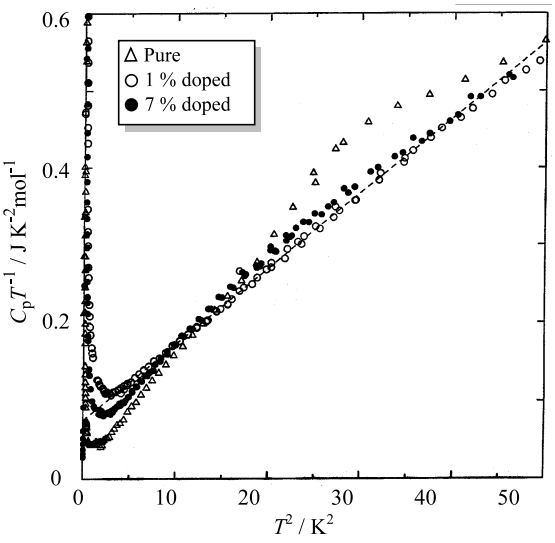

Fig. 4. C_P/T versus T^2 plot of the heat capacity of the 0, 1 and 7% doped p-CyDOV crystals. The dashed line represents the fit of Eq. (4) to the experimental values for the estimation of the lattice contribution of the heat capacity.

The main contribution to the heat capacity comes from the lattice and the magnetic systems. In the 7% doped p-CyDOV, the SP transition disappears and the susceptibility has the characteristics of a quasi 1D Heisenberg AFM with $S = 1/2$ and with $2J/k_B = -81.1$ K (see Table 1) [19]. Consequently, at low temperatures $T > T_N = 0.164$ K, the magnetic heat capacity, C_M, may vary as $0.35Nk_B^2T/|J|$, as expected for the quasi-1D Heisenberg AFM in the temperature region $T < 0.2|J|/k_B \cong 8$ K [18,27]. Then the total heat capacity in this temperature region may be expressed as

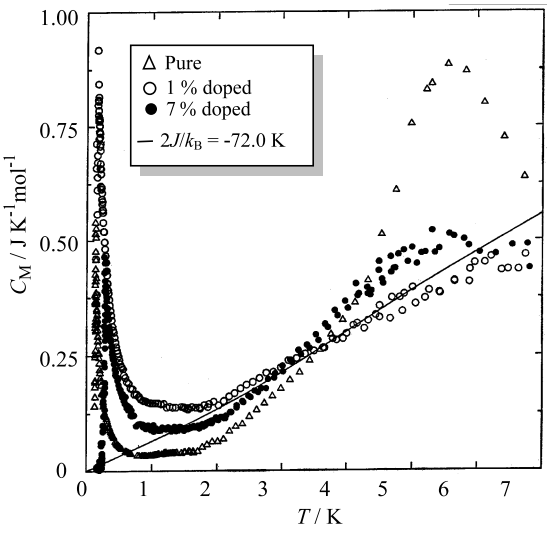

Fig. 5. C_M versus T plot of the magnetic heat capacities of the 0, 1 and 7% doped p-CyDOV crystals in the temperature range of 0.10–7 K.

$$C_P = C_M + C_L = 0.35 N_A k_B^2 T/|J| + A(\theta_D) T^3 \quad (4)$$

where N_A is Avogadro's number and θ_D is the Debye temperature for the lattice contribution C_L. Here we comment that impurities act to cut the 1D chain into 1D segments of average length of 14 lattice points for $x = 0.07$. It is noted, however, that the experimental results fit well to the C_P/T versus T^2 plot, as shown in Fig. 4. From the straight line in Fig. 4, we can estimate $|J|/k_B = 36.0$ K and $A(\theta_D) = 9.75 \times 10^{-3}$ J (mol K^4)$^{-1}$, making a correction for the 1D segments of finite length. The lattice heat capacity, C_L, thus obtained is exhibited in Fig. 3. The value of $2J/k_B$ (−72.0 K) obtained shows good accordance with that (−81.1 K) obtained from the magnetic susceptibility measurement [19].

On the other hand, the total heat capacities for the crystals with $x = 0$ and 0.01 deviate from Eq. (4), as shown in Fig. 4, because they are in the SP phase in this temperature region. We assume that the lattice heat capacities of the pure and doped p-CyDOV crystals with $x = 0$ and 0.01 are the same as that for $x = 0.07$, because the molecular structures of the p-CyDOV and p-CyDTV are similar to each other, and the crystal structures of the doped crystals ($x = 0$, 0.01, and 0.07) have the same crystal symmetry, as was studied by the X-ray analysis [19]. In fact, the overall heat capacities are nearly common at high temperature region, as shown in Fig. 2. Therefore, subtracting this lattice contribution from the total heat capacity yields the magnetic heat capacity, C_M, of the pure and 1% doped p-CyDOV in the temperature region $T < 7$ K, which is exhibited in Fig. 5. C_M of the 7% doped crystal shows a λ-type peak at $T_N = 0.164$ K and increases linearly above 2 K due to the contribution from 1D Heisenberg AFM. On the other hand, C_M of the pure p-CyDOV crystal shows an appearance of a broad peak at $T'_{SP} =$ 5.6 K in addition to the λ-like peak at $T_N = 0.135$ K, while C_M of the 1% doped crystal shows the intermediate behavior between those of the pure and 7% doped crystals above $T_N = 0.290$ K, also showing a broad peak at $T'_{SP} = 5.3$ K. We will discuss the broad peak later including its magnetic field dependence.

4. Discussion

4.1. AFM transition at $T_N(x)$ in the pure and doped SP transition compounds and $T_N(x)$–x phase diagram

As shown in Fig. 3, the AFM orderings were observed for the pure and doped p-CyDOV crystals ($x = 0$, 0.01, and 0.07) at $T_N = 0.135$, 0.290, 0.164 K, respectively. If the pure p-CyDOV sample ($x = 0$) is an ideal SP crystal without imperfection, we cannot expect AFM ordering. Strictly speaking, however, the present p-CyDOV crystal is not an ideal crystal, and includes 0.4% Curie impurities due to terminals of the chain or lattice defects [19]. Therefore, the heat capacity peak at $T_N = 0.135$ K is also considered to indicate the AFM transition arising from the inevitable minute impurities.

The transitions for $x = 0$ and 0.01 are different from that for $x = 0.07$ from the x dependence of $T_N(x)$. The fact that $T_N(0.01) = 0.290$ K is enhanced by more than twice of $T_N(0) = 0.135$ K suggests that each spin state for these two concentrations is not in a simple quasi-1D magnet, where $T_N(x)$ drastically decreases by increasing x [28]. This contradiction is reasonably understood when we regard that the spin states for $x = 0$ and 0.01 are almost in the nonmagnetic SP phase, and that the doped impurities gives an effect to grow local magnetic moments around impurities enough to make appearance of the 3D ordering triggered by the small inter-chain interaction at the respective $T_N(x)$. That is, in the SP phase, the more the impurities, the more the growth of the moments, giving the enhancement of $T_N(x)$. It should be noted here that the heat capacities for $x = 0$ and 0.01, when compared with the case for $x = 0.07$, drop quite steeply as in the exponential decrease below $T_N(x)$, suggesting a coexistence of some gap phase in the 3D magnetic ordered phase. Theoretically the growth of the local magnetic moments in the doped SP phase has been pointed out by Fukuyama et al. [29] for instance. The occurrence of the AFM ordering in the SP phase was also reported in the Mg-doped $CuGeO_3$ with small impurities less than $x_C = 0.023$ [12].

On the other hand, the concentration $x = 0.07$ is supposed to be larger than the critical concentration x_C for which the local magnetic moments are dominant enough to disrupt the SP phase at all temperatures, where the impurities act to cut the 1D chain into shorter segments. This is the reason for the reduction of $T_N(x)$ for $x = 0.07$. That is, the high temperature phase above

$T_N(0.07) = 0.164$ K is merely a paramagnetic state of a quasi-1D chain of about 14 lattice points.

Transition temperature vs impurity concentration (T–x) phase diagrams have been reported on Zn- [9], Mg- [12], Ni- [30], and Si- [15] doped $CuGeO_3$ systems. In Zn- and Si-doped $CuGeO_3$ systems, Neel temperature (T_N) increases gradually, reaches its maximum, and decreases moderately, by increasing x. The T_{SP} decreases linearly as x increases, and disappears suddenly at the critical concentration x_C. A first-order phase transition between dimerized-AFM and uniform-AFM phases has been reported for the Mg-doped SP system, $Cu_{1-x}Mg_xGeO_3$ [12]. As Mg concentration increases, linear reduction of the SP transition temperature (T_{SP}) and linear increase of the Neel temperature (T_N) are observed for x up to $x_C \sim 0.023$. At x_C, the SP transition suddenly disappears, and T_N jumps discontinuously and decreases gradually by increasing x. These results indicate the existence of a first-order phase transition between dimerized-AFM and uniform-AFM long-range orders. Similar behavior was observed for the Ni-doped $CuGeO_3$ system [30].

One of the most interesting phenomena observed in these doped $CuGeO_3$ systems is the coexistence of the long-range order of the lattice dimerization, which is intrinsic to SP phase, and the AFM long-range order. The neutron scattering experiments were performed for Zn- [9] and Si- [13,14] doped $CuGeO_3$, and both dimerization superlattice peak and AFM peak were observed. Fukuyama et al. [29] theoretically explained the coexistence of the dimerization and the AFM long-range order in $CuGe_{1-x}Si_xO_3$ using phase Hamiltonian. According to their theory, the coexistence of the dimerization and $\langle S^Z \rangle$ of spins on Cu^{2+} ions with spatially inhomogeneous distribution has been suggested. Recent μSR study [10] on Zn- and Si-doped $CuGeO_3$ indicated the spatial inhomogeneity of $\langle S^Z \rangle$ of spins on Cu^{2+} ions in AFM long-range order phase, which supports the theory of Fukuyama et al.

Fig. 6 shows p-CyDTV concentration dependence of T_{SP} and T_N: T–x phase diagram. As observed for the doped $CuGeO_3$, T_{SP} of the doped p-CyDOV system decreases linearly as x increases, and disappears at $x =$ 0.02–0.03 [19]. T_N increases from $T_N = 0.135$ K at $x = 0$ to $T_N = 0.290$ K at $x = 0.01$, and then decreases to $T_N =$ 0.164 K at $x = 0.07$. It should be noted here that the temperature axis is indicated with the logarithmic scale to demonstrate the low temperature region. The overall T–x phase diagram is qualitatively the same as in the doped $CuGeO_3$ systems. The result suggests the coexistence of the SP phase and the AFM long-range order in the doped p-CyDOV systems with small impurity concentration x.

The inter-chain interaction $|zJ'|$ in the present organic SP system was estimated as follows: the doped p-CyDOV system with $x = 0.07$ showed the uniform-

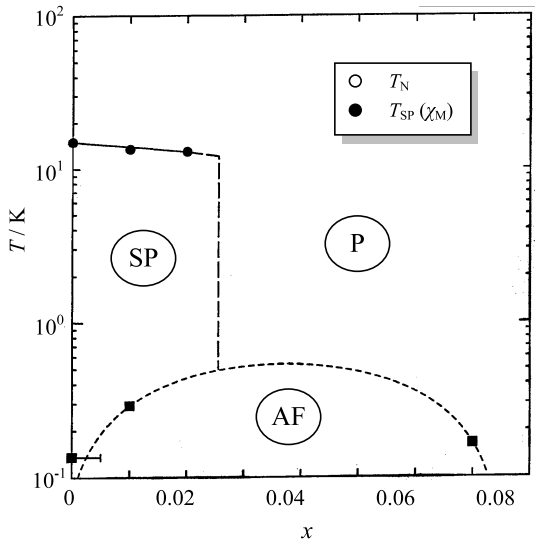

Fig. 6. The T–x phase diagram of the doped p-CyDOV crystals, $(p\text{-CyDOV})_{1-x}(p\text{-CyDTV})_x$, obtained from the magnetic susceptibility (T_{SP}) and heat capacity (T_N) measurements. Closed circles and closed squares indicate T_{SP} and T_N, respectively. SP, AF and P indicate SP, AFM and paramagnetic states, respectively.

AFM transition at $T_N = 0.164$ K. From the mean field theory, T_N is expressed as $k_B T_N \cong 2S^2\xi_{1D}|zJ'|$ [31], where ξ_{1D} is the 1D AFM correlation length in the chain. For $x = 0.07$, the value of ξ_{1D} is cut at around 13, and $2J/k_B = -81.1$ K as listed in Table 1. The value of $|zJ'/J| \approx 6 \times 10^{-4}$ obtained from the above equation is much smaller than that (10^{-1}) for $CuGeO_3$, indicating a high one-dimensionality in the p-CyDOV system. This is a main reason for the low AFM transition temperatures in the present organic system.

The temperature dependence of the magnetic entropies, $S_M(T)$'s, for the pure and doped crystals ($x = 0$, 0.01, and 0.07) was obtained from the relation

$$S_M(T) = \int_0^T (C_M(T)/T)\mathrm{d}T \quad (5)$$

$S_M(T)$ at the lowest temperatures is approximated by extrapolating the experimental value of C_M down to 0 K with 3D spin-wave approximation, namely, with a series expansion starting from T^3 term. At any rate, $S_M(T_O)$ at the lowest T_O for the present data points is fairly small for $S_M(\infty) = R \ln 2 = 5.635$ JK^{-1} mol^{-1}. For the 7% doped crystal, about 21% of the magnetic entropy ($R \ln 2$ for $S = 1/2$) is consumed up to 7 K, and the remaining 79% is expected at higher temperatures, as shown in Fig. 7. The critical entropy $S_M(T_N)$ up to T_N is about 10% of the total entropy $R \ln 2$. This is another reflection of the low-dimensionality of the magnetic interaction in p-CyDOV: the value of $S_M(T_N)$ is nearly 50% for the 2D localized spin systems, and in the usual 3D systems, $S_M(T_N)$ is rather close to $R \ln 2$ [24,32].

$S_M(T)$'s of the pure and 1% doped crystals are also shown in Fig. 7. The values of $S_M(T)$'s of these crystals

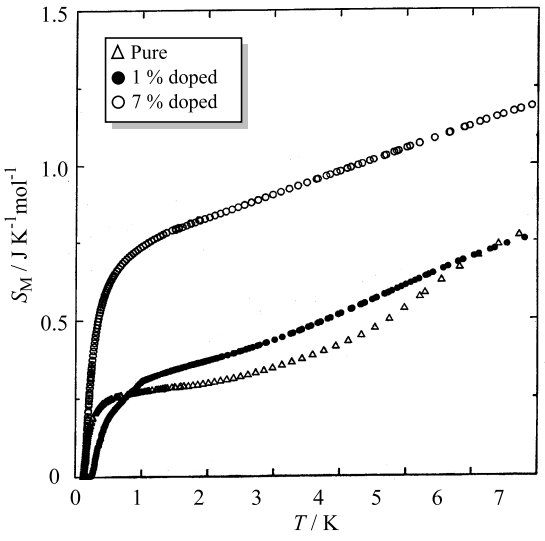

Fig. 7. Magnetic entropy ($S_M(T)$) of the doped p-CyDOV radical system ($x = 0$, 0.01 and 0.07).

below 7 K are nearly a half that of the 7% doped crystal, as expected [3]. It should be noted that the rapid consumption of the magnetic entropy at low temperatures is associated with the AFM transition and fairly gradual increase around 2 K indicates that the most spins are in the SP state.

4.2. Disappearance of heat capacity peak at $T_{SP}(x)$ and appearance of anomalous broad peak at $T'_{SP}(x)$ in the pure and 1% doped SP systems

Generally, the SP transition accompanies some anomalies in both magnetic and thermal quantities at the common SP transition temperature, as found at $T_{SP} = 12.4$ K for TTF-BDT (Cu) [26], $T_{SP} = 2.06$ K for TTF-BDT (Au) [26], $T_{SP} = 18$ K for MEM-(TCNQ)$_2$ [3], and $T_{SP} = 14$ K for $CuGeO_3$ [6]. Theχ_M of p-CyDOV crystal shows a broad maximum at 54 K, and decreases abruptly at $T_{SP} = 15.0$ K. The susceptibility above 15.0 K can be well described by the 1D Heisenberg linear chain model [16,19], as expected for the typical SP transition compounds. Further, high-field magnetization data ($H = 0$–35 T) that provide clear evidence for a SP transition were reported, and the magnetic phase diagram was determined for the p-CyDOV crystal [16,17,25]. However, we could not observe any heat capacity anomaly at the temperature (15.0 K).

If the abrupt decrease in the χ_M of p-CyDOV crystal is not due to the SP transition, but due to the first-order phase transition accompanying dimerization of the neighboring radical molecules, the heat capacity anomaly with large entropy change, which can not be explained by taking only the magnetic contribution, will be observed at 15.0 K, as reported for galvinoxyl radical [33,34] and Wurster's blue perchlorate [35,36]. However, such an anomaly was not observed for the p-CyDOV crystal, as described above.

On the other hand, as shown in Fig. 5, a broad peak was found in C_M around $T'_{SP} = 5.6$ K for the system with $x = 0$, and a weaker broad peak around 5.3 K with $x = 0.01$. The application of the external field makes shift the broad peak to the lower temperatures and smears out (the data are not shown). The result indicates that the broad peak is not due to the first-order phase transition. The entropy consumption in the broad peak for $x = 0$ is about 3% of the total spin entropy $R \ln 2$ and is similar to 2.6% consumed around $T_{SP} = 14$ K for $CuGeO_3$ as estimated from the data of heat capacity in Ref. [6], suggesting that this transition may relate to SP transition.

For the SP transition, a subtle balance is required between the magnetic energy gain due to the spin dimerization and the lattice energy loss due to distortion. The SP compound p-CyDOV is a molecular crystal. Generally, molecular crystals are thought to be 'soft crystal' because molecules are connected by weak van der Waals bond. We used Apiezon-N grease as the thermal binder for the heat capacity measurement. When the grease is solidified at low temperatures, it may induce local pressure in the crystal. That is, the solidification of the grease affects the above subtle balance, and induces large shift on the SP transition temperature from original T_{SP} to T'_{SP}. However, the detailed reason for the shift of the transition temperature is not clear at present.

5. Summary

We prepared the doped organic SP system, (p-CyDOV)$_{1-x}$(p-CyDTV)$_x$ ($x = 0$, 0.01, and 0.07), and measured the heat capacities ($T = 0.10$–32 K) to study the effect of magnetic impurities, p-CyDTV ($S = 1/2$), on the SP transition of p-CyDOV crystal ($S = 1/2$, $T_{SP} = 15.0$ K), where the $>C=O$ group in p-CyDOV is replaced by the $>C=S$ group in p-CyDTV. The AFM transitions ($T_N = 0.135$, 0.290, and 0.164 K) were observed for the doped crystals ($x = 0$, 0.01, and 0.07), respectively, indicating (i) the coexistence of dimerized-AFM order (D-AF) and SP state in the doped SP system with $x = 0$ and 0.01, and (ii) the appearance of uniform-AFM order (U-AF) in the doped system with $x = 0.07$ at low temperatures. The behavior is similar to that of doped inorganic SP system, $Cu_{1-x}M_xGeO_3$ (M = Zn, Mg, and Ni), although the doped organic SP system shows much higher one-dimensionality compared to that of doped $CuGeO_3$ system. Although the heat capacity anomalies expected for the pure and 1% doped p-CyDOV crystals were not observed at around $T_{SP} =$ 15.0 K, we observed a broad peak of the heat capacity at $T'_{SP}(0) = 5.6$ K and $T'_{SP}(0.01) = 5.3$ K with magnetic

entropy consumption up to about 3% of the total spin entropy $R \ln 2$. This value is similar to 2.6% consumed around $T_{SP} = 14$ K for $CuGeO_3$, suggesting that this transition may relate to SP transition. The pressure induced by the solidification of the Apiezon-N grease, which was used as the thermal binder for the heat capacity measurement, at low temperature may affect the shift of the SP transition temperature. This work is the first report of the heat capacity study of the doping effect on the organic SP transition system.

Acknowledgements

This work was supported by the Grant-in-Aid for Scientific Research on Priority Areas (B) of Molecular Conductors and Magnets (Area No. 730/11224205) from the Ministry of Education, Science, Sports and Culture, Japan.

References

[1] J.W. Bray, H.R. Hart, Jr., L.V. Interrante, I.S. Jacobs, J.S. Kasper, G.D. Watkins, S.H. Wee, J.C. Bonner, Phys. Rev. Lett. 35 (1975) 744.
[2] I.S. Jacobs, J.W. Bray, H.R. Hart, Jr., L.V. Interrante, J.S. Kasper, G.D. Watkins, D.E. Prober, J.C. Bonner, Phys. Rev. B 14 (1976) 3036.
[3] S. Huizinga, J. Kommandeur, G.A. Sawatzky, B.T. Thole, K. Kopinga, W.J.M. de Jonge, J. Roos, Phys. Rev. B 19 (1979) 4723.
[4] M. Hase, I. Terasaki, K. Uchinokura, Phys. Rev. Lett. 70 (1993) 3651.
[5] M. Hase, I. Terasaki, Y. Sasago, K. Uchinokura, Phys. Rev. Lett. 71 (1993) 4059.
[6] S.B. Oseroff, S.-W. Cheong, B. Aktas, M.F. Hundley, Z. Fisk, L.W. Rupp, Jr., Phys. Rev. Lett. 74 (1995) 1450.
[7] B. Grenier, J.-P. Renard, P. Veillet, C. Paulsen, G. Dhalenne, A. Revcolevschi, Phys. Rev. B 58 (1998) 8202.
[8] S. Elizabeth, P.K. Babu, H.L. Bhat, Solid State Commun. 106 (1998) 149.
[9] M.C. Martin, M. Hase, K. Hirota, G. Shirane, Y. Sasago, N. Koide, K. Uchinokura, Phys. Rev. B 56 (1997) 3173.
[10] K.M. Kojima, Y. Fudamoto, M. Larkin, G.M. Luke, J. Merrin, B. Nachumi, Y.J. Uemura, M. Hase, Y. Sasago, K. Uchinokura, Y. Ajiro, A. Revcolevschi, J.-P. Renard, Phys. Rev. Lett. 79 (1997) 503.
[11] Y. Ajiro, T. Asano, F. Masui, M. Mekata, H. Aruga-Katori, T. Goto, H. Kikuchi, Phys. Rev. B 51 (1995) 9399.
[12] Y. Masuda, A. Fujioka, Y. Uchiyama, I. Tsukada, K. Uchinokura, Phys. Rev. Lett. 80 (1998) 4566.
[13] L.P. Regnault, J.-P. Renard, G. Dhalenne, A. Revcolevschi, Europhys. Lett. 32 (1995) 579.
[14] J.-P. Renard, K. Le Dang, P. Veillet, G. Dhalenne, A. Revcolevschi, L.P. Regnault, Europhys. Lett. 30 (1995) 475.
[15] B. Grenier, J.-P. Renard, P. Veillet, C. Paulsen, R. Calemczuk, G. Dhalenne, A. Revcolevschi, Phys. Rev. B 57 (1998) 3444.
[16] K. Mukai, N. Wada, J.B. Jamali, N. Achiwa, Y. Narumi, K. Kindo, T. Kobayashi, K. Amaya, Chem. Phys. Lett. 257 (1996) 538.
[17] T. Hamamoto, Y. Narumi, K. Kindo, K. Mukai, Y. Shimobe, T.C. Kobayashi, T. Muramatsu, K. Amaya, Physica B 246–247 (1998) 36.
[18] J.C. Bonner, M.E. Fisher, Phys. Rev. A 135 (1964) 640.
[19] K. Mukai, Y. Yanagimoto, Y. Shimobe, K. Inoue, Y. Hosokoshi, Chem. Phys. Lett. 311 (1999) 446.
[20] J.B. Jamali, N. Wada, Y. Shimobe, N. Achiwa, S. Kuwajima, Y. Soejima, K. Mukai, Chem. Phys. Lett. 292 (1998) 661.
[21] K. Mukai, Y. Shimobe, J.B. Jamali, N. Achiwa, J. Phys. Chem. 103 (1999) 10876.
[22] K. Mukai, M. Yanagimoto, Y. Shimobe, K. Kindo, T. Hamamoto, J. Phys. Chem. B 106 (2002) 3687.
[23] F.A. Neugebauer, H. Fisher, R. Siegel, Chem. Ber. 121 (1988) 815.
[24] K. Takeda, Y. Yoshino, K. Matsumoto, T. Haseda, J. Phys. Soc. Jpn 49 (1980) 162.
[25] K. Mukai, M. Yanagimoto, H. Maruyama, Y. Narumi, K. Kindo, J. Phys. Soc. Jpn 71 (2002) 2539.
[26] T. Wei, A.J. Heeger, M.B. Salamon, G.E. Delker, Solid State Commun. 21 (1977) 595.
[27] K. Takeda, Y. Yoshino, K. Matsumoto, T. Haseda, J. Phys. Soc. Jpn 49 (1980) 162.
[28] K. Takeda, J.C. Schouten, J. Phys. Soc. Jpn 50 (1981) 2554.
[29] H. Fukuyama, T. Tanimoto, M. Saito, J. Phys. Soc. Jpn 65 (1996) 1182.
[30] N. Koide, Y. Uchiyama, T. Hayashi, T. Masuda, Y. Sasago, K. Uchinokura, K. Manabe, H. Ishimoto, Cond-mat/9805095.
[31] J. Villain, J.M. Loveluck, J. de Phys. Lett. 38 (1977) L77.
[32] L.J. de Jongh, A.R. Miedema, Adv. Phys. 23 (1974) 135.
[33] K. Mukai, Bull. Chem. Soc. Jpn 42 (1969) 40.
[34] A. Kosaki, H. Suga, S. Seki, K. Mukai, Y. Deguchi, Bull. Chem. Soc. Jpn 42 (1969) 1525.
[35] W. Duffy, Jr., J. Chem. Phys. 36 (1962) 490.
[36] H. Chihara, M. Nakamura, S. Seki, Bull. Chem. Soc. Jpn 38 (1965) 1776.